Bioprocess and Biosystems Engineering 24 (2002) 309–318
DOI 10.1007/s00449-001-0272-7

Comparative evaluation of various control schemes for fed-batch fermentation

Hisbullah, M.A. Hussain, K.B. Ramachandran

Abstract The crucial problem associated with control of fed-batch fermentation process is its time-varying characteristics. A successful controller should be able to deal with this feature in addition to the inherent nonlinear characteristics of the process. In this work, various schemes for controlling the glucose feed rate of fed-batch baker's yeast fermentation were evaluated. The controllers evaluated are fixed-gain proportional-integral (PI), scheduled-gain PI, adaptive neural network and hybrid neural network PI. The difference between the specific carbon dioxide evolution rate and oxygen uptake rate (Q_c–Q_o) was used as the controller variable. The evaluation was carried out by observing the performance of the controllers in dealing with setpoint tracking and disturbance rejection. The results confirm the unsatisfactory performance of the conventional controller where significant oscillation and offsets exist. Among the controllers considered, the hybrid neural network PI controller shows good performance.

Abbreviations

CER	Carbon dioxide evolution rate
min	minimum; a function
PI	Proportional-integral
OUR	Oxygen uptake rate
RQ	Respiratory quotient

List of symbols

C_i	concentration of component i, mol × l^{-1}
E	absolute error differentiation between process and model
e	error
F	feed rate, l × h^{-1}
k_c	proportional band
k_I	integral time
V	volume of the fermentor, l
$Y_{i/j}$	yield of component i on j, mol × mol^{-1}
Q_i	specific consumption or production rate, mol × C-mol^{-1} × h^{-1}
m	glucose consumption rate for the maintenance, mol × C-mol^{-1} × h^{-1}
k_La_i	volumetric mass transfer coefficient for component i, h^{-1}
K_i	saturation constant of component i, mol × l^{-1}
K_l	inhibition constant, mol × l^{-1}

Greek symbols

α, β, γ	adjustment law paramaters
μ	grade of membership function
μ_i	specific growth rate based on component i, h^{-1}
μ_{cr}	critical specific growth rate, h^{-1}
Δ	difference
δ	adaptive factor

Subscripts and superscripts

x	baker's yeast cell
s	glucose
e	ethanol
o	oxygen
c	carbon dioxide
f	feed
ox	oxidative
pr	production
*	interface
max	maximum
lim	limitation
red	reductive
up	uptake
t, $t+1$, $t-1$	sampling point, discrete time
e	ethanol
act	actual
sp	setpoint
pred	predicted
cor	corrected

1 Introduction

The main issue in operating fed-batch fermentation is the control of the substrate feed rate, i.e., which strategy is suitable for its control under all conditions. The problem encountered is mainly due to the time-varying characteristics of the process. During the process, its dynamics gain increases as the amount of cell in the culture increases. Hence, the controller designed should be able to give responses matching the changes in the process dynamics

Received: 15 June 2001 / Accepted: 12 September 2001
Published online: 27 November 2001

Hisbullah, M.A. Hussain, K.B. Ramachandran (✉)
Department of Chemical Engineering,
University of Malaya, 50603 Kuala Lumpur, Malaysia
E-mail: kbram@fk.um.edu.my
Tel.: +60-3-79675293
Fax: +60-3-79675319

gain and at the same time be able to deal with the inherent process nonlinearity.

Generally, strategies which have been developed in controlling feed rate of fed-batch fermentation can be divided into three categories, namely single optimal control, single feedback control, and hybrid control. In single optimal control strategy, the feed rate is adjusted by means of an optimal profile determined either offline (programmed control approach) or online (feedforward control approach). The determination of this optimal feed rate profile can be carried out by using the simplified material balance equations and optimization procedures [1, 2, 3, 4]. In single feedback control strategy, the regulation of the feed rate relies merely on the feedback control scheme. Early attempts on this strategy were made with PID controllers. Subsequently, motivated by nonlinearity and the modeling uncertainty of bioprocesses, other feedback approaches have been developed involving model-based adaptive schemes [5, 6]. Application of hybrid control strategies commonly involved optimal and feedback controllers. The optimal controller, either programmed or feedforward control approach, serves as the primary controller, while the feedback controller serves as the compensator [7, 8, 9].

During the past decade, the use of artificial neural networks in fed-batch fermentation control has grown significantly [10, 11]. Neural networks can represent complex nonlinear relationships and uncertainty as posed by the fed-batch fermentation process. The use of neural networks as state estimation, pattern recognition, fuzzy membership function adjustment, and parameter adaptation for the purpose of fed-batch fermentation control has been intensively studied [10]. However, the use of it as a direct controller has not been intensively explored yet. This is because there are difficulties encountered in formulating a neural network control model. Due to its time-varying characteristics, fed-batch fermentation requires substantial training data for the neural network control model to represent its dynamic behavior. Unfortunately, such a large amount of data is costly and difficult to obtain. Moreover, by using such a large number of data for training, the desired model with a small error is difficult and takes a long training time.

A gain-changing scheme has shown to be able to improve the performance of neural-network-based controllers for nonlinear processes by eliminating or reducing offsets. Schubert et al. [12] applied this scheme to adapt the hybrid neural-network model of the internal model controller (IMC) for a fed-batch yeast cultivation. The hybrid model was adapted online by additionally training it with small gains, in order to reduce the deviation between its estimation values and the values monitored at the plant. Dayal et al. [13] incorporated a gain-scheduling scheme in the neural-network internal model controller (NN-IMC) for a nonlinear continuous stirred-tank reactor (CSTR). This scheme was aimed at correcting for the control action of the neural-network controller in order to eliminate the steady-state offsets of the controlled variable due to the discrepancy between the inverse model of the neural-network controller and the internal neural-network model.

In this work, we used an adaptive scheme using a fuzzy-logic method to improve the performance of an inverse neural-network controller for fed-batch baker's yeast fermentation. A hybrid strategy involving neural-network and PI controllers was proposed to improve the performance further. The performance of these neural-network-based controllers are compared to fixed- and scheduled-gain proportional-integral (PI) controllers. The control objective was to obtain optimum productivity and yield of baker's yeast by regulating the glucose feed rate. To regulate the glucose feed rate, the difference between the specific carbon dioxide evolution rate and oxygen uptake rate (Q_c–Q_o) was chosen as the controlled variable.

2
Baker's yeast fermentation

Optimizing productivity and yield is essential in baker's yeast fermentation. This issue emerges because a conflict exists between the two. If glucose is excessively available in the culture, the productivity is high, but the yield is low. In contrast, if the culture lacks glucose, the productivity is low, but the yield is high. According to Sonnleitner and Kappeli [14], three different metabolic pathways take place during baker's yeast fermentation. They are oxidation of glucose (R1), reduction of glucose (R2), and oxidation of ethanol (R3). These pathways are governed by the respiratory capacity of the cells. If the substrate flux is less than the respiratory capacity of the cells, both pathway R1 and pathway R3 are active with priority for pathway R1. Pathway R2 is active only if the glucose flux exceeds the respiratory capacity of the cells. Glucose flux is high when its residual concentration in the fermentation medium is high. Conversely, glucose flux is low when its residual concentration is low. Hence, the need to control the residual concentration of glucose in the fermentation medium at a level which will give glucose flux matching the respiratory capacity of the cells.

Although, all the pathways result in cell production, the pathway R2 is economically undesirable because it leads to ethanol formation which results in low baker's yeast yield. One cannot rely on pathway R3 to utilize all the ethanol formed because part of it may be carried out of the fermentor along with aeration gases due to its volatility. The way to overcome this productivity and yield conflict is by accurately regulating the glucose feeding in such a way that it ensures the glucose concentration is tightly maintained in the state where only pathway R1 occurs and the respiratory capacity of the cells are utilized to the maximum.

3
Control variable selection

Since glucose concentration is the main factor affecting the switching among the various pathways mentioned above, its regulation is important, but it is a state variable which is difficult to measure [6]. Besides, its measurement does not give any indication as to how the glucose is channeled through different pathways. Ethanol concentration in the culture, which can be easily measured by gas chromatography, can be also used to observe the switching of the pathways. The best variable which gives indication of switching of pathways in baker's yeast fermentation is the

respiratory quotient (RQ). The respiratory quotient (RQ) is the ratio of the carbon dioxide evolution rate (CER) to the oxygen uptake rate (OUR). RQ greater than 1 indicates ethanol formation and RQ in the range 0.9–1.0 indicates oxidative growth. Although using RQ as a controlled variable showed some success in some studies, control quality has been limited in the sense that glucose concentration in the culture is not tightly maintained at the optimal value [15]. This is because an RQ value around 1.0 does not mean the full utilization of the respiratory capacity of the cells through pathway R1.

In this study, we used the difference between specific CER and OUR, i.e., Q_c–Q_o, as a controlled variable by regulating the glucose feed rate. The use of the specific quantities enables Q_c–Q_o to be held constant and independent of the increasing change in biomass during fermentation. Since the control variables involve specific values, besides measuring CER and OUR, biomass concentration also needs to be measured. This can be achieved by sensors [16] and various estimation methods such as neural networks that have been developed [12, 17]. Unlike ethanol concentration and RQ, Q_c–Q_o has a unique value for the state of the full utilization of the respiratory capacity of cells through pathway R1. Figure 1 illustrates this point.

Figure 1 was generated by computer simulation based on the model reported by Pertev et al. [18]. The same model was used to evaluate the performance of the various controllers. The model and its parameter values are given in Table 1 and Table 2, respectively. The profile of the feed rate was adjusted in such a way that the activation of the three pathways could be observed, as shown by the change in glucose and ethanol concentrations in the culture during fermentation. At around 3 h, it can be seen that the ethanol concentration is just beginning to rise from zero value. At this point, the respiratory capacity of the cells is fully utilized for glucose oxidation. At this state, RQ is equal to 1.083 and the value of Q_c–Q_o is 0.0062. At the later part of the fermentation, i.e., after 7 h, even when the respiratory capacity is not fully utilized for glucose oxidation, the RQ value remains constant at 1.083, but a variation in Q_c–Q_o is observed. Hence, RQ equals 1.083 does not mean that the respiratory capacity of the cells is fully utilized. However, if the magnitude of Q_c–Q_o is equal to 0.0062, it means the respiratory capacity of the cells is fully utilized for glucose oxidation. Below this value means it is not fully utilized for glucose oxidation. In baker's

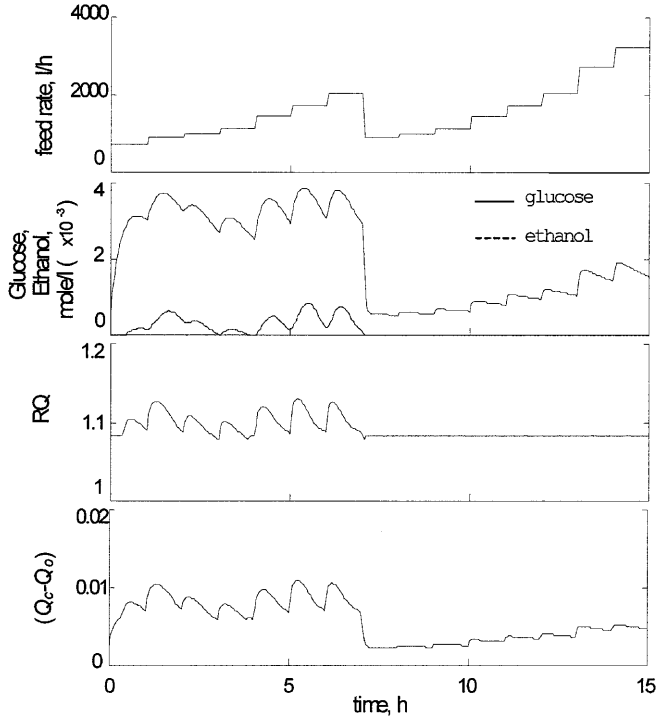

Fig. 1. Changes in ethanol concentration, the respiratory capacity (RQ), and the dierence between specific carbon dioxide evolution rate and oxygen uptake rate (CER-OUR) due to varying glucose feed rate

Table 1. Process model used in the simulation study

Balance equations

$$dC_x/dt = (\mu_x - F/V)C_x$$
$$dC_s/dt = (F/V)\left(C_s^f - C_s\right) - \left(\left(\mu_s/Y_{x/s}^{ox}\right) + \left(Q_e^{pr}/Y_{e/s}\right) + m\right)C_x$$
$$dC_e/dt = -(F/V)C_e^f + \left(Q_e^{pr} - Q_e^{ox}\right)C_x$$
$$dC_o/dt = -(F/V)C_o^f - Q_oC_x + k_La_o\left(C_o^* - C_o\right)$$
$$dC_c/dt = -(F/V)C_c^f + Q_cC_x + k_La_c\left(C_c^* - C_c\right)$$
$$dV/dt = F$$

Rate equations

$$Q_s = Q_s^{\max}(C_s/(K_s + C_s))$$
$$Q_o^{\lim} = Q_o^{\max}(C_o/(K_o + C_o))$$
$$Q_s^{\lim} = \mu_{cr}/Y_{x/s}^{ox}$$
$$Q_s^{ox} = \min\left(\left[\left(Q_s\right); \left(Q_s^{\lim}\right); \left(Y_{o/s}Q_o^{\lim}\right)\right]\right)$$
$$Q_s^{\text{red}} = Q_s - Q_s^{ox}$$
$$Q_e^{up} = Q_e^{\max}(C_e/(K_e + C_e))(K_l/(K_l + C_s))$$
$$Q_e^{ox} = \min\left(\left[\left(Q_e^{up}\right); \left(\left(Q_o^{\lim} - Q_s^{ox}Y_{o/s}\right)Y_{o/e}\right)\right]\right)$$
$$Q_e^{pr} = Y_{e/s}Q_s^{\text{red}}$$
$$\mu_x = Y_{x/s}^{ox}Q_s^{ox} + Y_{x/s}^{\text{red}}Q_s^{\text{red}} + Y_{x/e}Q_e^{ox}$$
$$\mu_s = Y_{x/s}^{ox}Q_s^{ox} + Y_{x/s}^{\text{red}}Q_s^{\text{red}}$$
$$Q_c = Y_{c/s}^{ox}Q_s^{ox} + Y_{c/s}^{\text{red}}Q_s^{\text{red}} + Y_{c/e}Q_e^{ox}$$
$$Q_o = Y_{o/s}Q_s^{ox} + Y_{o/e}Q_e^{ox}$$
$$RQ = Q_c/Q_o$$

Table 2. Parameter values for the process model [18]

Parameters	Values
m	0.00321 mol × C-mol^{-1} × h^{-1}
K_e	0.008 mol × l^{-1}
K_l	0.001 mol × l^{-1}
K_o	0.000003 mol × l^{-1}
K_s	0.002 mol × l^{-1}
$Q_e^{\max}$	0.70805 mol × C-mol^{-1} × h^{-1}
$Q_o^{\max}$	0.20 mol × C-mol^{-1} × h^{-1}
$Q_s^{\max}$	0.06 mol × C-mol^{-1}h^{-1}
μ_{cr}	0.15753 h^{-1}
$Y_{x/e}$	2.0 mol × mol^{-1}
$Y_{c/e}$	0.68 mol × mol^{-1}
$Y_{o/e}$	1.28 mol × mol^{-1}
$Y_{e/s}$	1.9 mol × mol^{-1}
$Y_{o/s}$	2.17 mol × mol^{-1}
$Y_{c/s}^{ox}$	2.35 mol × mol^{-1}
$Y_{c/s}^{\text{red}}$	1.89 mol × mol^{-1}
$Y_{x/s}^{ox}$	4.570636 mol × mol^{-1}
$Y_{x/s}^{\text{red}}$	0.1 mol × mol^{-1}
C_c^*	0.00001 mol × l^{-1}
C_o^*	0.000241 mol × l^{-1}
k_La_o	600 h^{-1}
k_La_c	470.4 h^{-1}

yeast fermentation, respiratory capacity of the cells should be used fully to maximize productivity. Hence, Q_c–Q_o is a better control parameter than RQ for regulating glucose feed rate. It should be noted that, due to its small magnitude, the Q_c–Q_o value may be affected by noisy measurement. However, experimental results show that noises in carbon dioxide measurement are small enough, i.e., within 0.01%, and the same range applies for oxygen measurement as well [19]. Also biomass concentration can be estimated with only a small error and hence, it is reasonable to conclude that the use of Q_c–Q_o is practically viable. In spite of this, in practice, an effective noise filter is still recommended.

4 Simulation study

In this work, the fed-batch baker's yeast fermentation process was simulated using the model given in Table 1. The length of fermentation time was fixed at 15 h and the sampling time interval was 0.05 h. The process was initiated with the following conditions: 0.54 mol $\times$ l^{-1}, 5×10^{-4} mol $\times$ l^{-1}, 2.41×10^{-4} mol $\times$ l^{-1}, and 0 mol $\times$ l^{-1} for cell, glucose, ethanol, oxygen, and carbon dioxide concentrations in the culture, respectively, and 50,000 l for volume of the fermentor. In the first 0.90 h of the operation, the glucose, whose concentration in the feed was 1.6 mol $\times$ l^{-1}, was added to the fermentor according to a predetermined profile. Then, at t=0.90 h, the controller was activated. The control objective was to obtain optimum productivity and yield of baker's yeast by tightly controlling the glucose feed rate to the culture to maintain the Q_c–Q_o value at 0.0062.

The controllers studied were PI controllers with fixed- and scheduled-gain schemes and neural-network-based controllers with single adaptive and hybrid schemes. The performance of the controllers was evaluated by observing the process responses through setpoint tracking for the nominal value of Q_c–Q_o at 0.0062 and disturbance rejection studies. The disturbance was the change in glucose concentration in feed stream from its nominal value of 1.6 mol $\times$ l^{-1}. The disturbance was introduced at t=2.0, 5.0, 7.5, 10.0, and 12.5 h with the value of the glucose concentration changed to 1.7, 1.5, 1.7, 1.5, and 1.6 mol $\times$ l^{-1}, respectively. The control action was constrained within the range of 0 to $\pm$750 l $\times$ h^{-1} for practical reasons.

5 Results and discussion

5.1 Fixed-gain PI controller

The algorithm of the controller is as follows:

$$\Delta F_{t+1} = k_c\left(e_t - e_{t-1} + \frac{\Delta t}{k_I} e_t\right) \tag{1}$$

$$e_t = (Q_c - Q_o)_{sp} - (Q_c - Q_o)_t \tag{2}$$

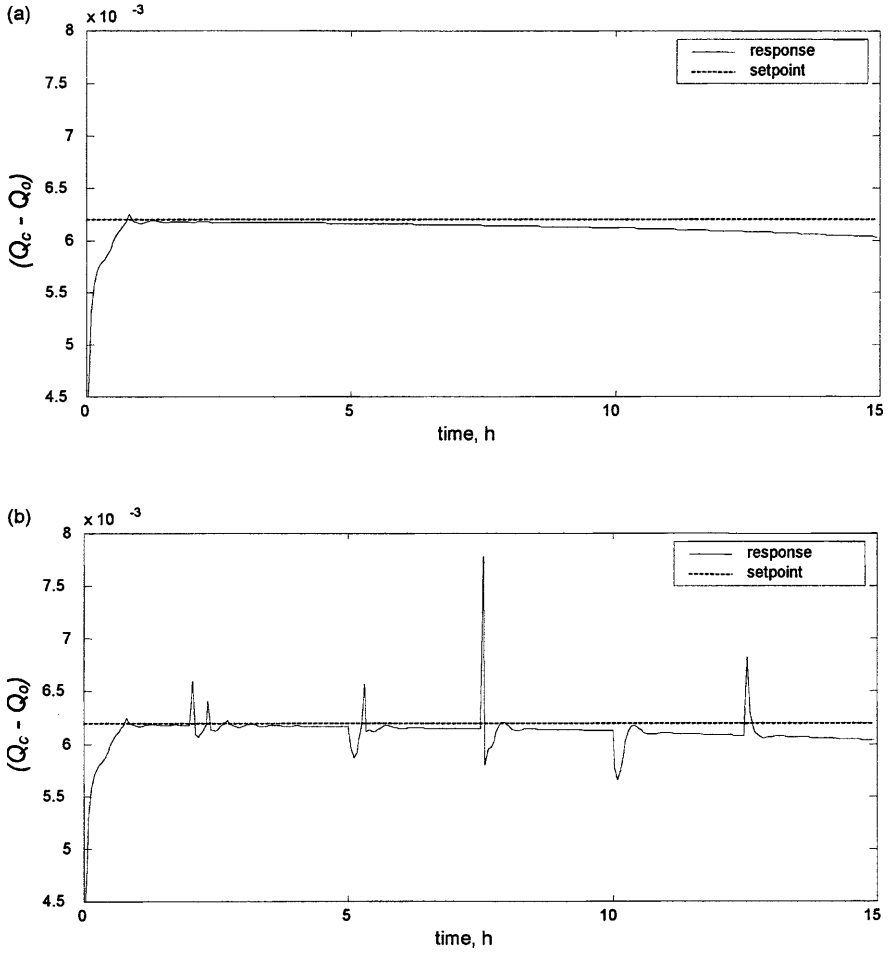

Fig. 2a, b. Response of the fixed-gain PI controller for **a** nominal setpoint tracking and **b** disturbance rejection

$$F_{t+1} = F_t + \Delta F_{t+1} \quad (3)$$

The controller parameters, k_c and k_I, were determined by means of trial and error and the best result is presented here, i.e., for tuning values of 400 and 0.00007 for k_c and k_I, respectively. The values are fixed throughout the fermentation. The performance of the controller for the setpoint tracking and disturbance rejection is shown in Fig. 2.

From Fig. 2a, we can see that in the early period after control was implemented, i.e., from t = 0.90 to t = 1.5 h, the controller is able to track the setpoint in a reasonable manner. Further to this, offset is observed below the setpoint with increasing magnitude. In Fig. 2b, significant oscillation is observed when the controller responds to the disturbances in the early period of the process, i.e., in the first 7.5 h operation. It can been seen that the response of the controller is faster when the deviation is negative (above the setpoint) compared to that of positive (below the setpoint). Generally, it can be pointed out that the performance of this fixed-gain PI controller is poor due to the existence of offset.

5.2
Scheduled-gain PI controller

For this controller, the values of k_c and k_I in Eq. 1 were scheduled according to linearized segments. The fermentation process was divided into three segments, whose time lengths were 5 h each. For the first, second, and third period, the k_c and k_I settings were set at 400 and 0.0001; 450 and 0.00007; and 550 and 0.00005, respectively. The performance of the controller for the setpoint tracking and disturbance rejection is shown in Fig. 3.

Figure 3a shows that the PI controller with scheduled-gain scheme results in better performance in tracking the setpoint compared to that with fixed-gain (Fig. 2a). It can be seen that the offset is reduced in every segment, i.e., at t = 5 h and t = 10 h, as the gain of the controller is improved. This improvement also resulted in faster response. Nevertheless, as a consequence, it lead to some oscillation as observed at t = 10 h and t = 12.5 h.

5.3
Adaptive neural-network controller

The neural-network model used for the controller is the inverse form of the process. Details of neural networks and their various control strategies can be found elsewhere [20, 21, 22]. The model has three input nodes, consisting of the current difference in the value of the feed rate, the current and the future values of Q_c–Q_o, while the output is the future difference in the value of feed rate. The hidden layer has four nodes, whose number was determined by trial and error. The architecture of the model is shown in Fig. 4. The notations in the model are expressed by Eqs. 4, 5, 6, and 7.

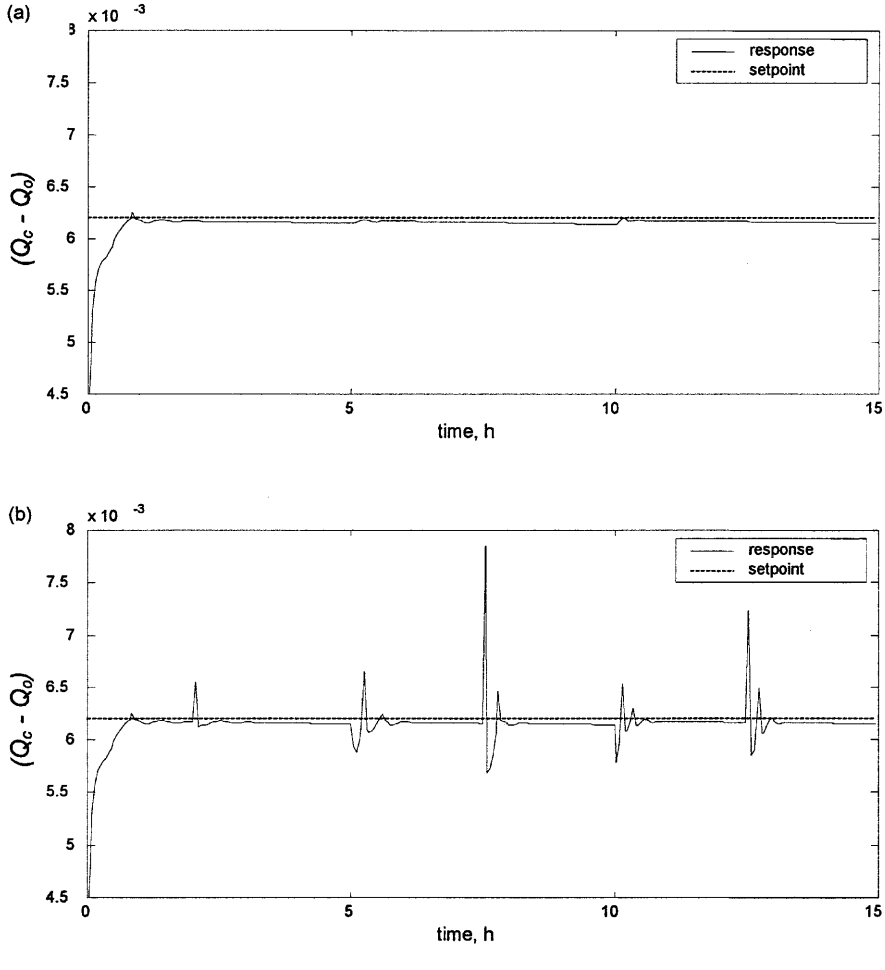

Fig. 3a, b. Response of the scheduled gain PI controller for **a** nominal setpoint tracking and **b** disturbance rejection

$$\Delta F_t = F_t - F_{t-1} \tag{4}$$

$$\Delta F_{t+1} = F_{t+1} - F_t \tag{5}$$

$$\Delta(Q_c - Q_o)_t = (Q_c - Q_o)_t - (Q_c - Q_o)_{t-1} \tag{6}$$

$$\Delta(Q_c - Q_o)_{t+1} = (Q_c - Q_o)_{t+1} - (Q_c - Q_o)_t \tag{7}$$

Using two sets of batch data, the model was trained using a sigmoidal function for nodes in the hidden layer and a linear function for the output node. In implementation, the $(Q_c - Q_o)_{t+1}$ in Eq. 7 serves as the setpoint, while the control action is the F_{t+1} obtained from Eq. 5.

Due to the architecture of the model and the lack of training data, the control based on this model resulted in poor performance, as shown in Fig. 5. It can be seen that the controller induced severe oscillation in the first half of the period of operation and had offset in the later period. Hence, to improve the performance of the controller, we incorporated an adaptive factor for the output of the model.

By this scheme, the adaptive factor α serves as a gain correcting the output of the controller F_{t+1} in order to match the gain of the process along the operation. The adaptive control law is expressed as follows:

$$F_{t+1,\mathrm{cor}} = \delta . F_{t+1} \tag{8}$$

The concentration of the cells in the culture was used to determine the adaptive factor using a fuzzy-logic method. The method involves fuzzy membership functions for the concentration of biomas constituting fuzzy sets of low, medium, high, and very high as shown in Fig. 6 and fuzzy rules established by the Sugeno fuzzy inference method [20]. The adaptive factors are given in the equation below.

$$\begin{aligned} &\text{If } X \text{ is } \textit{low} \text{ then } \delta = 0.35\mu \\ &\text{If } X \text{ is } \textit{medium} \text{ then } \delta = 0.9\mu \\ &\text{If } X \text{ is } \textit{high} \text{ then } \delta = 1.5\mu \\ &\text{If } X \text{ is } \textit{very} \text{ high then } \delta = 2.1\mu \end{aligned} \tag{9}$$

X and μ are biomass concentration and grade of fuzzy membership function, respectively. Performance of the neural-network controller with this adaptive scheme for the nominal setpoint tracking and disturbance rejection is shown in Fig. 7.

In Fig. 7a, it can be seen that the controller performed well for nominal setpoint tracking. A very small offset was observed in the beginning as soon as the controller was activated. Compared to the performance of the unadapted controller model in Fig. 5, we can point out that the adaptive scheme works well. In Fig. 7b, no oscillations and offsets are observed when the controller rejects the disturbances. However, slow response is

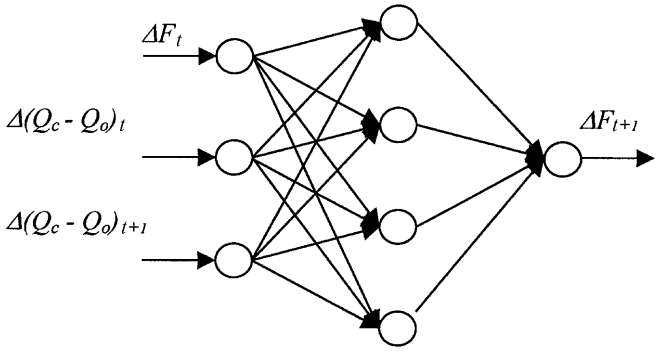

Fig. 4. The inverse neural-network model for control

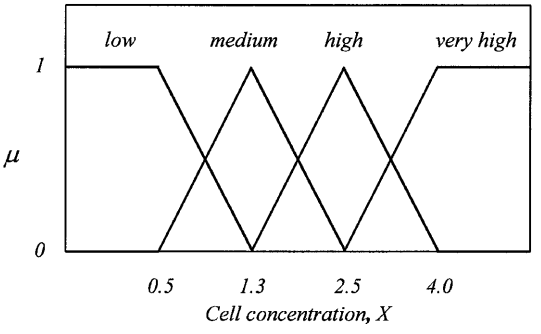

Fig. 6. Fuzzy membership function for biomass concentration

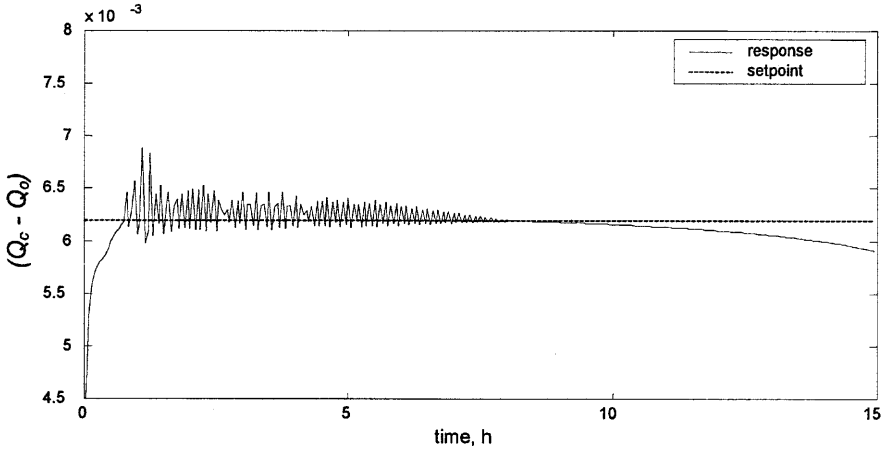

Fig. 5. Response of the process controlled by the poorly modeled neural-network controller for nominal setpoint tracking

observed. Compared to the fixed-gain PI controller (Fig. 2b) and the scheduled-gain controller (Fig. 3b), this controller results in a longer time for the controlled variable to settle.

5.4 Hybrid neural-network PI controller

Looking back at the previous control strategies we can conclude that the scheduled-gain PI controller produces fast response, but results in oscillations and offsets. On the other hand, the adaptive neural-network controller is slow in response, but it does not result in oscillations and offsets. Hence, we combined the merits of these two controllers into a hybrid control scheme, i.e., the hybrid neural-network PI controller.

In this hybrid controller, the neural-network controller serves as the main controller. It provides control actions directly based on the output of the process. The process response of this control action is then predicted by a model installed in parallel with the process. In case the predicted process response action indicates deviations from the setpoint, the PI controller will make correction for it by introducing a compensation signal. The hybrid control scheme is shown in Fig. 8.

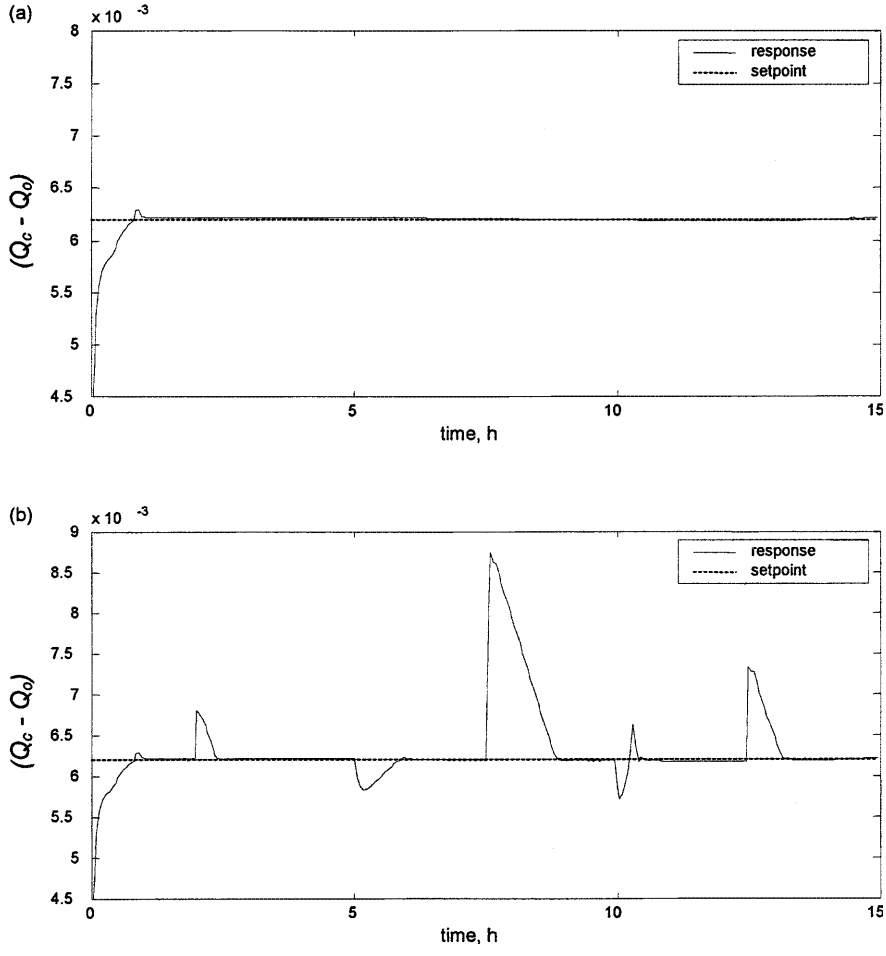

Fig. 7a, b. Response of the adaptive neural-network controller for **a** nominal setpoint tracking and **b** disturbance rejection

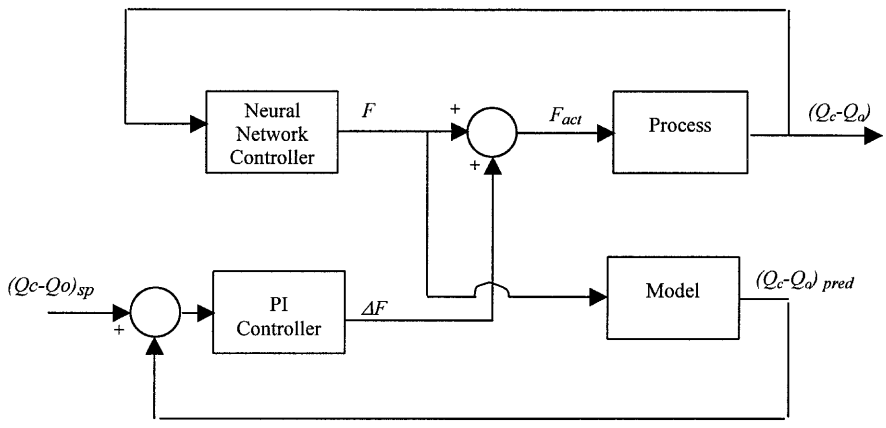

Fig. 8. Hybrid neural-network PI controller

Since the control scheme is model based, the controller may cause slight error in the compensation signal when model mismatch occurs during the process. For this reason, it is reasonable to reduce the gain of the PI controller in the case of model mismatch. This is achieved by decreasing k_c and increasing k_I (see Eq. 1), with the relative model mismatch error as the reference parameter. The reduction law is expressed as follows:

$$k_c' = k_c(a - E)/\alpha;\ \alpha \geq E_{\max} \tag{10}$$

$$k_I' = k_I(\beta E);\ E \geq E_{\min} \text{ and } \beta \geq 1/E_{\min} \tag{11}$$

where

$$E = \left|(y_p - y_m)/y_m\right| \tag{12}$$

k_c' and k_I' represent the reducted values of k_c and k_I. α and β denote the reducing factors for k_c and k_I, respectively. E, $E_{\max}$, and $E_{\min}$ represent the relative model mismatch error, its estimated maximum value, and its minimum value, respectively. y_p and y_m represent the process and model outputs, respectively.

Figure 9 shows the performance of the controller for nominal setpoint tracking and disturbance rejection. The values for k_c and k_I are set at 400 and 0.0001, respectively, for first 7.5 h and 400 and 0.00007, respectively, for the rest. From Fig. 9a, it can be noted that the controller performance is satisfactory from the start. No oscillations and offsets are observed. The setpoint is tracked correctly. Figure 9b shows the merits of the scheduled-gain PI and the adaptive neural-network controllers when they are combined properly. The controller is able to reject the disturbances with fast response with no offset except for t=7.5 h, where offset with oscillations are observed.

Robustness of the controller is illustrated in Fig. 10. It shows the response of the process to the variation in $Q_s^{\max}$ (its nominal value is 0.060 mol × C-mol^{-1} × h^{-1}). The parameter varies with values of 0.065, 0.057, 0.063, 0.055, and 0.065 mol × C-mol^{-1} × h^{-1} at operation times of 2.5, 5, 7.5, 10, and 12.5 h, respectively. Figure 10a shows the process response with setting values for α, β, and E_{min} of 0.75, 200, and 0.005, respectively. It can be seen that when the effect of model mismatch is large (large E), sluggish process response with oscillations is observed (t = 2.5–5 h and t = 7,5–10 h). In these periods, the gain of the PI controller gets reduced in such a way that the compensation signal resulting from the controller is small and so the neural-network controller dominates the control action. When the effect of model mismatch is low (low E), the reduced gain still makes the PI controller significant to give contribution to control action. Because the PI controller works based on the predicting model, it produces an over-compensating signal as a result of erroneous predicted process output when model mismatch occurs.

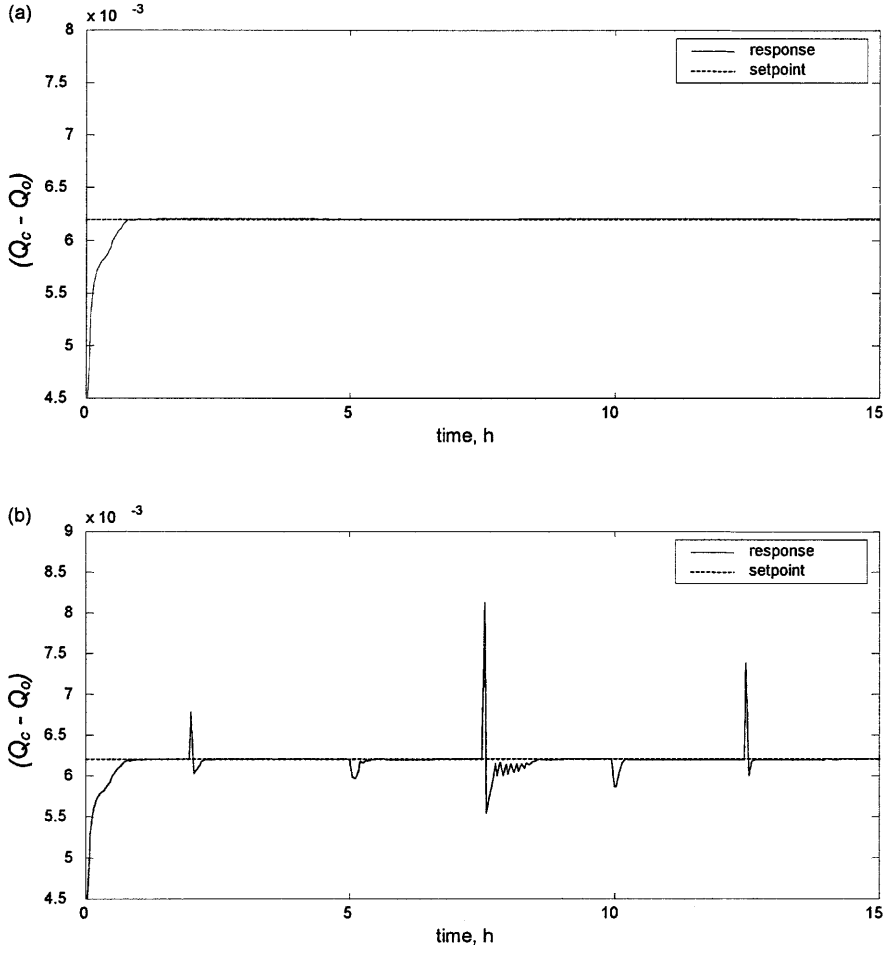

Fig. 9a, b. Response of the hybrid neural-network and PI controller for **a** nominal setpoint tracking and **b** disturbance rejection

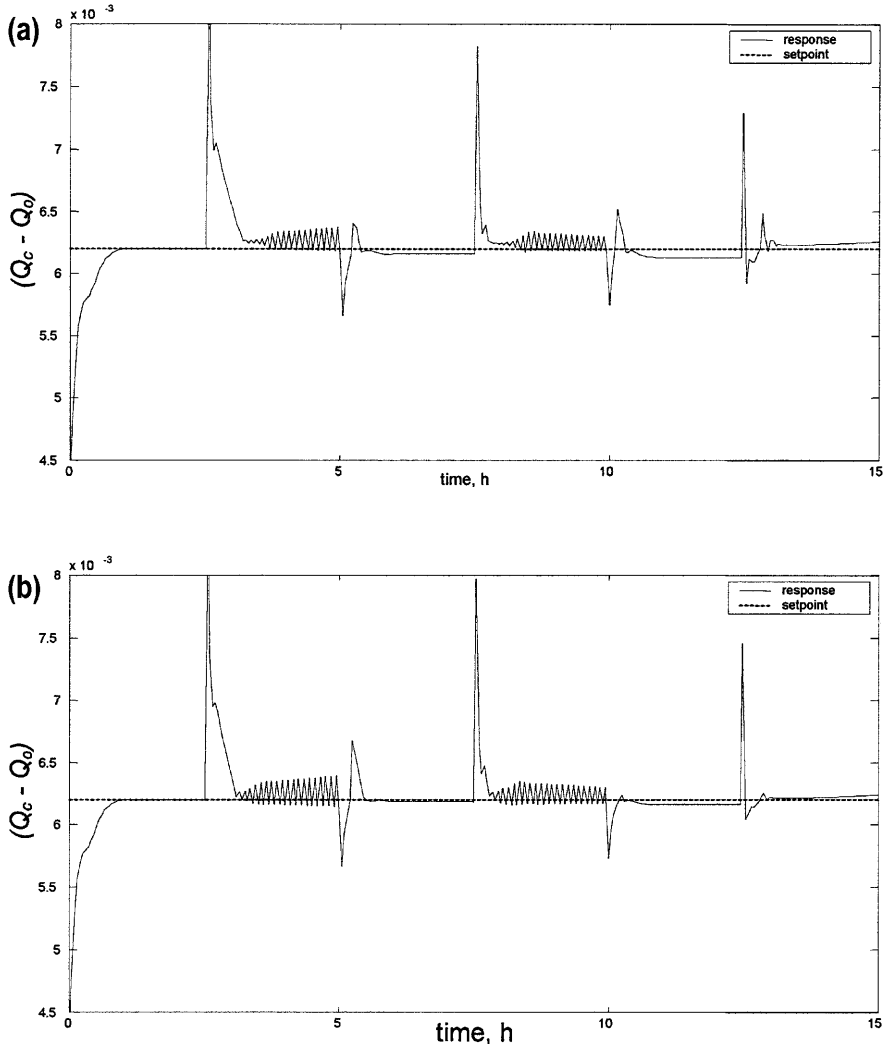

Fig. 10a, b. Response of the hybrid neural-network and PI controller for model mismatch with **a** $\alpha = 0.75$, $\beta = 200$, $E_{min} = 0.05$; **b** $\alpha = 0.5$, $\beta = 400$, $E_{min} = 0.005$

Such a signal will result in offsets in process response, as observed in the figure in the periods of $t = 5$–7.5, $t = 10$–12.5 h, and $t = 12.5$–15 h. The offsets can further be minimized, i.e., by setting the value of α to 0.5 and the value of β to 400. The result for this is shown in Fig. 10b. From this study, it can be seen that the proposed controller can take care of model mismatch reasonably well and is fairly robust.

6 Conclusion

The crucial problem in controlling a fed-batch fermentation is that the process exhibits time-varying and nonlinear characteristics. Oscillations and offset are features controllers should overcome. This study shows that conventional control strategies, as represented by the fixed-gain PI controller, result in unsatisfactory performance. It also demonstrates that control schemes with simple adaptive methods, as represented by the scheduled-gain PI and the adaptive neural-network controllers, are also unable to solve this problem. Hybrid control schemes appear to be one of the answers to overcome this. Hybrid neural-network PI controller performance is relatively better in overcoming the oscillation and offsets with fast response and short settling time for setpoint tracking and disturbance rejection compared to the three previously mentioned control strategies. Model mismatches are dealt with by this controller by reducing the gain of the PI controller so as to prevent it from producing over-compensating signal when model mismatch occurs. By setting proper parameters for the reduction law, reasonable robustness can be achieved, which makes it viable for online implementation.

References

1. Aiba S, Nagai S, Nishizawa Y (1976) Fed-batch culture of *Saccharomyces cerevisiae*: a perspective of computer control to enhance the productivity in baker's yeast cultivation. Biotechnol Bioeng 18:1001–1016
2. Wang HY, Cooney CL, Wang DIC (1979) Computer control of baker's yeast production. Biotechnol Bioeng 21:975–995
3. Johnson A (1987) The control of fed-batch fermentation processes: a survey. Automatica 23:691–705
4. O'Connor GM, Riera FS, Cooney CL (1992) Design and evaluation of control strategies for high-cell-density fermentations. Biotechnol Bioeng 39:293–304
5. Boskovic JD, Narendra KS (1995) Comparison of linear, nonlinear and neural network- based adaptive controllers for a class of fed-batch fermentation processes. Automatica 31:817–840

6. Chen L, Bastin G, Breusegem B Van (1995) A case study of adaptive nonlinear regulation of fed-batch biological reactors. Automatica 1:55–65
7. Dairaku K, Izumoto E, Morikawa H, Shioya S, Takamatsu T (1983) An advanced micro-computer coupled control system in a baker's yeast fed-batch culture using a tubing method. J Ferment Technol 61:189–196
8. Takamatsu T, Shioya S, Okada Y (1985) Profile control scheme in a baker's yeast fed-batch culture. Biotechnol Bioeng 27:1675–1686
9. Park YS, Shi ZP, Shiba S, Chantal C, Iijima S, Kobayashi T (1993) Application of fuzzy reasoning to control of glucose and ethanol concentrations in baker's yeast culture. Appl Microbiol Biotechnol 38:649–655
10. Lee J, Lee SY, Park S, Middelberg APJ (1999) Control of fed-batch fermentations. Biotechnol Adv 17:29–48
11. Rani KY, Rao VSR (1999) Control of fermenters: a review. Bioprocess Eng 21:77–88
12. Schubert J, Simutis R, Dors M, Havlik I, Lubbert A (1994) Bioprocess optimization and control: application of hybrid modeling. J Biotechnol 35:51–68
13. Dayal BS, Taylor PA, Macgregor JF (1994) The design of experiments, training and implementation of nonlinear controllers based on neural networks. Can J Chem Eng 72:1066–1079
14. Sonnleitner B, Kappeli O (1986) Growth of *Saccharomyces cerevisiae* is controlled by its limited respiratory capacity: formulation and verification of a hypothesis. Biotechnol Bioeng 28:927–937
15. Shimizu K, Morikawa M, Mizutani S, Iijima S, Matsubara M, Kobayashi T (1988) Comparison of control techniques for baker's yeast culture using an automatic glucose analyzer. J Chem Eng (Jap) 21:113–117
16. Montague G (1997) Monitoring and control of bioreactors. Institution of Chemical Engineers, UK
17. Albiol J, Campmajo C, Casas C, Poch M (1995) Biomass estimation in plant cell cultures: a neural network approach. Biotechnol Prog 11:88–92
18. Pertev C, Turker M, Berber R (1997) Dynamic modeling, sensitivity analysis and parameter estimation of industrial yeast fermenters. Comput Chem Eng 21:S739–S744
19. Nilsson A, Taherzadeh MJ, Liden G (2001) Use of dynamic step response for control of fed-batch conversion of lignocellulosic hydrolyzates to ethanol. J Biotechnol 89:41–53
20. Tsoukalas LH, Uhrig RE (1997) Fuzzy and neural approaches in engineering. Wiley, Chichester
21. Aziz N, Hussain MA, Mujtaba IM (2000) Optimal control of batch reactors using generic model control (GMC) and neural network. In: Pierucci S (ed) Proceedings of The 10th European Symposium on Computer-Aided Process Engineering, 2000, Elsevier Science, Amsterdam, p 175
22. Aziz N, Hussain MA, Mujtaba IM (2000) Performance of different types of controllers in tracking optimal temperature profiles in batch reactors. Comput Chem Eng 24:1069